PLOS ONE

RESEARCH ARTICLE

A normative database of A-scan data using the Heidelberg Spectralis Spectral Domain Optical Coherence Tomography machine

Joos Meyer[1☯*], **Roshan Karri**[2☯], **Helen Danesh-Meyer**[3,4‡], **Kate Drummond**[3,5‡], **Andrew Symons**[1,3,6,7,8‡]

1 Ophthalmology Department, The Royal Melbourne Hospital, Parkville, VIC, Australia, **2** The Faculty of Medicine, Dentistry and Health Sciences, The University of Melbourne, Parkville, VIC, Australia, **3** Department of Surgery, The University of Melbourne, Parkville, Victoria, Australia, **4** Department of Ophthalmology, New Zealand National Eye Centre, University of Auckland, Auckland, New Zealand, **5** The Royal Melbourne Hospital, Neurosurgery Department, Parkville, VIC, Australia, **6** Centre For Eye Research Australia, East Melbourne, VIC, Australia, **7** Department of Optometry and Vision Sciences, The University of Melbourne, Parkville, Victoria, Australia, **8** Monash University Department of Surgery, Monash Medical Centre Level 5, North Melbourne, Australia

☯ These authors contributed equally to this work.
‡ These authors also contributed equally to this work.
* joos.meyer@mh.org.au

Citation: Meyer J, Karri R, Danesh-Meyer H, Drummond K, Symons A (2021) A normative database of A-scan data using the Heidelberg Spectralis Spectral Domain Optical Coherence Tomography machine. PLoS ONE 16(7): e0253720. https://doi.org/10.1371/journal.pone.0253720

Editor: Demetrios G. Vavvas, Massachusetts Eye & Ear Infirmary, Harvard Medical School, UNITED STATES

Received: March 21, 2021

Accepted: June 10, 2021

Published: July 1, 2021

Data Availability Statement: The data is held in figshare repository with DOI: 10.6084/m9.figshare.14794839.

Funding: The author(s) received no specific funding for this work.

Competing interests: The authors have declared that no competing interests exist.

Abstract

Purpose

To develop the first normative database of macular and circumpapillary scans with reference values at the level of the A-scan using the Heidelberg Spectralis Optical Coherence Tomography (OCT) machine.

Methods

This study is a retrospective cross sectional analysis of macular and circumpapillary OCT scans of healthy individuals. All participants had a full ophthalmic examination, including best corrected visual acuity, intraocular pressure, biomicroscopy, posterior segment examination and OCT scan. The volume and thickness of each of the nine Early Treatment Diabetic Retinopathy zones at the macula were analysed for the total retinal thickness, retinal nerve fibre layer (RNFL), ganglion cell layer (GCL) and inner plexiform layer (IPL). The thickness of the circumpapillary RNFL was analysed at the disc. Associations between age, gender, refractive error and OCT measurements were explored. De-identified A-scans were extracted from the OCT machine as separate tab-separated text file and made available according to the data sharing statement.

Results

Two-hundred eyes from 146 participants were included of which 69 (47%) were female. The mean age (SD) was 48.52 (17.52). Participants were evenly distributed across four age groups and represented nine broad ethnic groups in proportions comparable to the local distribution. All the macular scans were 20˚ x 20˚ (5.9 mm x 5.9 mm), with a total scan density

between 12,800 and 49,152 A-scans. The peripapillary scans were all 12˚ (3.5 mm), at a scan density of 768 A-scans. The mean retinal, GCL and IPL volumes were significantly greater in males than females. Mean peripapillary RNFL thickness did not differ significantly between males and females. Age and total retinal volume (r = –0.2561, P = 0.0003), GCL volume (–0.2911, P < 0.0001) and IPL volume (–0.3194, P < 0.0001) were negatively correlated. The IPL had the strongest three significant negatively associated segments; superior inner IPL (r = –0.3444, P < 0.0001), nasal outer IPL (r = –0.3217, P < 0.0001) and inferior inner IPL (r = –0.3179, P < 0.0001). The temporal inner macular RNFL showed a statistically significant positive correlation (r = 0.1929, P = 0.0062) with age. The only significant association between age and thickness at the peripapillary disc scan was the superior temporal sector (r = –0.1910, P = 0.0067). All retinal layers were negatively correlated for refractive error, except for the central RNFL which was positively correlated (r = 0.1426, P = 0.044).

Conclusion

This study provides a normative database of macular and circumpapillary scans with reference values at the level of the A-scan using the Heidelberg Spectralis Optical Coherence Tomography (OCT) machine.

Introduction

Optical coherence tomography (OCT) is a non-invasive imaging technology that uses low coherence interferometry to create two-dimensional cross-sectional imaging of biological systems [1]. In ophthalmic practice, OCT is used to image and measure the retinal architecture and changes that occur in disease states. Diseases, such as glaucoma and compressive optic neuropathy, manifest distinct changes on OCT scans, particularly on the inner retinal layers. Important OCT measurements for both diseases include the circumpapillary retinal nerve fibre layer (RNFL), macular RNFL and the macular ganglion cell layer (GCL) [2, 3].

The Early Treatment Diabetic Retinopathy Study (ETDRS) grid is a standardised pattern of dividing and measuring the thickness and volume profile of the retina [4]. It was first introduced in 1980, and is still the primary method of reporting [5]. Since its inception, additional grid patterns have been developed; [6] however, there is limited flexibility for clinicians and researchers to explore novel patterns of segmentation within any currently commercially available software.

For the macular, the standard 20˚ x 20˚ scan consists of horizontally stacked scan lines to create a square scan area. Each horizontal line is termed a B-scan, and each of these comprises a row of equally distanced A-scans. The A-scan represents the most basic unit of interrogation from which the rest of the scan is generated. The scan density of the Heidelberg Stratus (Heidelberg Engineering, Heidelberg, Germany) varies between 25,000 and 50,000 A-scans. For the optic disc, the standard circumpapillary scan consists of a 360˚ radial scan of 720 A-scans. Extracting the A-scan data enables the exploration of OCT changes that do not conform to the spatial distribution of the predefined grid patterns.

A normative database of scans is needed for comparison to validate changes in disease states. To the author's knowledge, a normative database that contains both macular and circumpapillary scans, which includes reference values for each A-scan of the Heidelberg Stratus, does not currently exist.

The purpose of this study is to report the normative values for macular and optic disc scans within the standard ETDRS grid and at the level of the A-scan. This study aims to help clinicians and researchers to identify patterns of change that occur outside the standard segmentation patterns of the retina.

Methods

Study population

This study is a retrospective cross-sectional analysis of 200 normal eyes that had a visual assessment and an OCT scan. The participants included patients of The Royal Melbourne Hospital (RMH) who were found to have no ocular pathology or systemic disease that could manifest in retinal changes. The RMH database was used to create this normative database. Approximately 50,000 eyes have been scanned since 2012 on the Heidelberg Spectralis machine at The RMH. The database was queried for normal OCT scans, and the potential participant's medical records were checked against inclusion and exclusion criteria. All of the participants had a full ophthalmic examination, including their Snellen best corrected visual acuity (BCVA), intraocular pressure (IOP), biomicroscopy, posterior segment examination and OCT scan. The participant's medical records were examined for any exclusions.

The retrospective inclusion criteria included healthy participants, aged 18 to 88, with a BCVA of 6/12 (20/40) on the Snellen chart measured at 6 m (20 feet), and high quality macular and peripapillary OCT scans (signal strength >15dB). The exclusion criteria included a history of any: (i) anterior segment disease (except cataracts); (ii) retinal disease; (iii) glaucoma; (iv) uveitis; (v) optic nerve disease; (vi) systemic disease known to affect the retina (e.g., diabetes); (vii) neurological disease; (viii) pituitary disease; (ix) intracranial space-occupying lesions; (x) previous neurosurgery; (xi) retinal lasers; (xii) vitrectomy; (xiii) topical or systemic anti-vascular endothelial growth factor treatment; (xix) IOP lowering medications; (xx) chemotherapy; or (xxi) previous systemic or active topical steroid use. The excluding biomarkers included peripapillary atrophy, RNFL haemorrhage, optic disc notching or thinning, age-related macular degeneration (including drusen) or macular disease on OCT scans. Ethnicity data were collected from the participants and categorised according to the Australian Bureau of Statistics' (ABS) Australian Standard Classification of Cultural and Ethnic Groups (ASCCEG) [7].

This study was approved by the Human Research and Ethics Committee of The RMH. It was conducted according to the Declaration of Helsinki in its currently applicable version.

Optical coherence tomography

All the OCT scans were performed with the Heidelberg Spectral is Spectral Domain (SD) OCT and the Heidelberg Eye Explorer version 6.7.13.0 (Heidelberg Engineering, Heidelberg, Germany). All scans were completed by experienced medical imaging personnel at The RMH medical imaging department; they were performed in a dark room as per the standard hospital protocol. Only the well-centred scans (>15dB quality) were included in the analysis. The focus in dioptres (spherical) was recorded for each scan as a proxy for the refractive error. The scans were quality controlled for the accurate segmentation of each macular retinal inner layer and peripapillary scan, and an experienced grader (JM) manually corrected any aberrations.

The macular scans were divided into 1 mm, 3 mm and 6 mm rings on the macular ETDRS map. The inner ring was defined as the central thickness, and the middle and outer rings were divided into four zones designated as the superior, nasal, inferior and temporal zones. The average thickness in each of the nine zones, the macular thickness and the full 360˚ peripapillary scans were included in the final analysis.

A-scan data

The A-scans were extracted from the machine using the Heidelberg Spectralis Layer Segmentation Export Special Function version 6.0. Each file contained the results from the automatic retinal layer segmentation algorithm of a Spectralis OCT machine as a tab-separated text file. The distance values of each A-scan location were represented as relative coordinates in nanometres from the probe to the layer segmentation interface. The normative values of the A-scans were compiled as a de-identified single data array per patient, per eye.

Statistical analysis

All analyses were conducted in the R statistical programming language using RStudio version 1.3.1073 (Boston, USA) [8]. The exploratory data analysis and data visualisation were performed using the ggplot2 package [9]. The descriptive statistics were reported as the mean, standard deviation and the first, fifth and 95th percentiles. An independent t-test was used to compare the thickness values between groups. The correlation between measurements was found using Pearson correlation coefficients. A multivariate analysis was used to consider the effects of age and gender; an alpha of 0.05 was considered significant. The chi-square goodness of fit test was used to compare the observed distribution of ABS ethnicities to the expected distribution in Melbourne, Australia.

Results

Study participants

Two-hundred eyes from 146 participants were included in the final analysis. There were 69 (47%) females and 77 (53%) males, and the mean age (SD) was 48.52 (17.52) (range: 21–85). Mean (SD) scan focus was 0.29 D (1.96) (range: -6.48–7.86). The participants were evenly distributed across the age groups (Table 1). Females were slightly under-represented in the younger age groups and over-represented in the older age groups. This study included 101 (50.5%) right eyes and 99 (49.5%) left eyes. Participants from nine broad ethnicity groups were included in the study (Table 2). There were significant differences in the proportion of broad ethnic categories compared to the census population proportions in North African and Middle Eastern, Oceanian, Southern and Central Asian and Sub Saharan African groups.

A-scans. Two-hundred de-identified tab separated text files were exported from the Heidelberg Stratus SD OCT machine. All the macular scans were 20˚ x 20˚ (5.9 mm x 5.9 mm), with 25 to 96 B-scans, and 512 A-scans per B-scan with the automatic real-time mode active. The total scan density was between 12,800 and 49,152 A-scans. The peripapillary scans were all 12˚ (3.5 mm diameter), at a scan density of 768 A-scans. All the scan data are available, according to the data sharing statement.

Table 1. Distribution of participants by age group and gender.

Age group	Participants, n (%)	Eyes, n (%)	Females, n (%)
18–33	37 (25.3)	52 (26.0)	14 (37.8)
34–50	41 (28.0)	62 (31.0)	13 (31.7)
51–68	43 (29.5)	57 (28.5)	27 (62.8)
69–88	25 (17.1)	29 (14.5)	15 (60.0)

https://doi.org/10.1371/journal.pone.0253720.t001

Table 2. Australian Bureau of Statistics Australian Standard Classification of Cultural and Ethnic Groups broad group classification of participants.

Broad ethnicity category	Participants, n (%)	Melbourne (%)	P
North African and Middle Eastern	15 (7.5)	1.9	<0.001
Northeast Asian	4 (2)	5.1	0.0644
Northwest European	9 (4.5)	5.3	0.7283
Oceanian	111 (55.5)	68.5	<0.001
People of the Americas	2 (1)	0.8	1
Southeast Asian	14 (7)	6.0	0.644
Southern and Central Asian	22 (11)	6.9	0.031
Southern and Eastern European	15 (7.5)	4.5	0.0666
Sub Saharan African	8 (4)	1.0	<0.001

https://doi.org/10.1371/journal.pone.0253720.t002

Distribution of macular and circumpapillary measurements

The mean (SD) total retinal volume was 8.67 mm^3 (0.38) (range: 7.65–9.58). The macular RNFL volume (SD) was 0.96 mm^3 (0.11) (range: 0.72–1.26). The GCL volume (SD) was mm^3 1.09 (0.10) (range: 0.82–1.31) and the inner plexiform layer (IPL) volume (SD) was 0.89 mm^3 (0.07) (range: 0.7–1.05). See Figs 1 and 2 demonstrating layer measurement distributions.

Difference in measurements between males and females

The multivariate regression analysis controlling for age and ethnicity (Table 3) showed that the retinal and GCL volumes were significantly less for females. The total RT was significantly lower in females in all sectors except for the superior outer sector. The same was true for the central, nasal inner, temporal inner, inferior inner macular RNFL, GCL and IPL thicknesses. The GCL and IPL also showed that females had significantly lower superior inner sectors. There were no significant differences found at the peripapillary RNFL between males and females S1 Table.

Decrease in thickness per decade

The mean retinal, GCL and IPL volumes were found to be significantly greater in males than females S2 Table. The mean volumes, ETDRS segment thickness values and the first, fifth and 95th percentile values were grouped by age for each macular layer (Tables 4–7). The mean (SD) peripapillary RNFL thickness was 99.7 μm (9.47) (range: 78–137). The mean peripapillary RNFL thicknesses were grouped by age (Table 8).

Linear regression analysis showed a significant negative correlation between the total retinal volume and age (r = –0.2561), GCL volume and age (–0.2911) and IPL volume and age (–0.3194). There was no significant correlation found between the RNFL and age. Figs 3 and 4 demonstrate trend lines for layer measurements against age. S3 Table demonstrates the regression analysis of segmental retinal thickness (RT) values against age. The strongest three significant negative associations were found in the superior inner IPL (r = –0.3444), nasal outer IPL (r = –0.3217) and inferior inner IPL (r = –0.3179) segments. The only significant positively correlated segment was the temporal inner RNFL (r = 0.1929). The only significant association between age and thickness at the peripapillary disc scan was the superior temporal sector (r = –0.1910) S4 Table.

Association between refractive error and thickness

Retinal thickness segments, except for the nasal outer, were not significantly correlated with refractive error. Nasal outer (r = -0.2020) and inferior outer (r = -0.1570) RNFL segments were

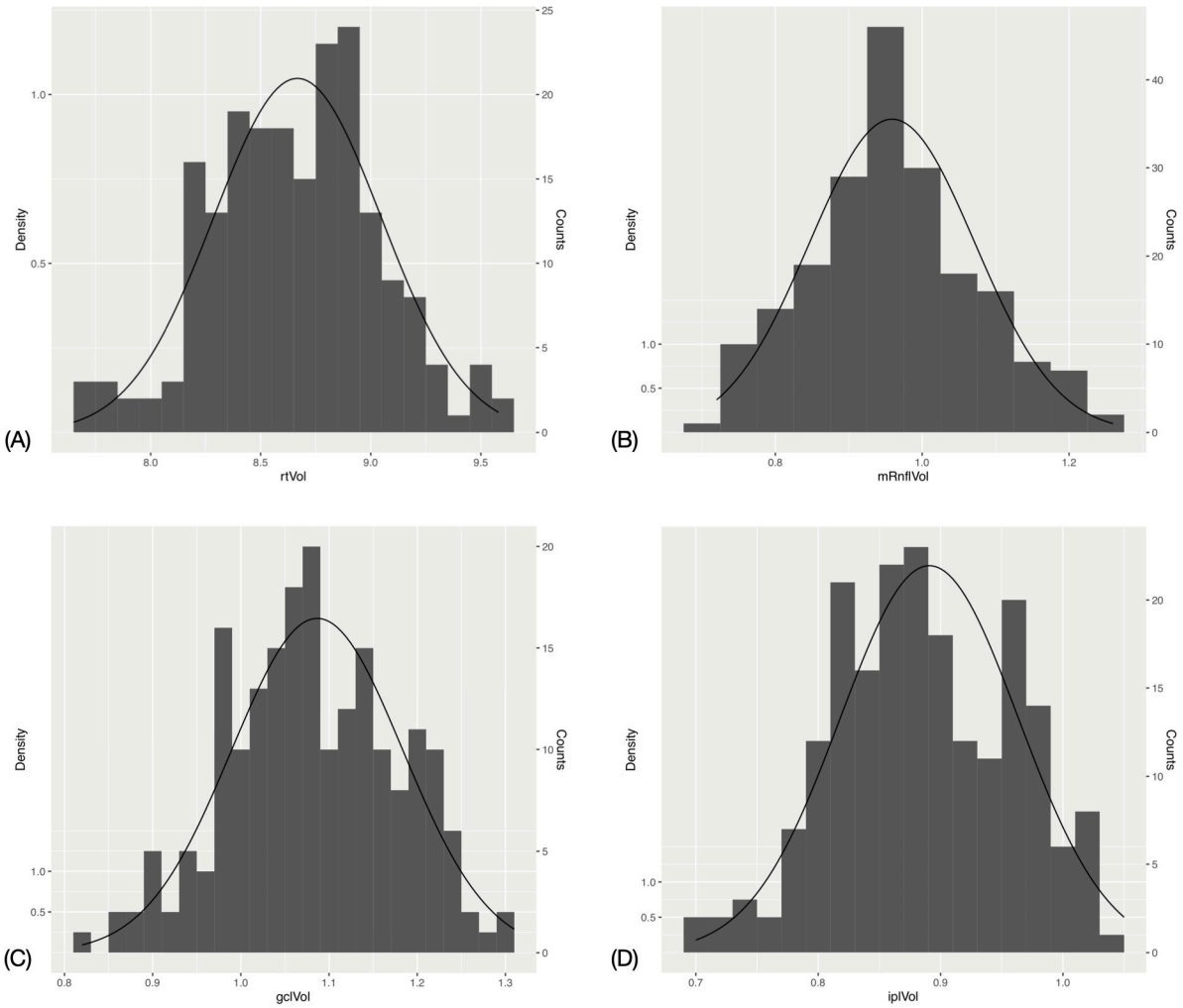

Fig 1. Histogram and fitted normal distribution curves of macular optical coherence tomography measurements. (A) Total retinal volume. (B) Retinal nerve fibre layer volume. (C) Ganglion cell layer volume. (D) Inner plexiform layer volume.

https://doi.org/10.1371/journal.pone.0253720.g001

negatively correlated. Central RNFL was positively correlated (r = 0.1426). GCL segments were only negatively correlated; superior inner (r = -0.2034), nasal inner (r = -0.1782), temporal inner (r = -0.1534) and nasal outer (r = -0.1478). The IPL had the most segments significantly correlated with refractive error all of which were negative and included IPL volume (r = -0.1668), nasal inner (r = -0.2154), nasal outer (r = -0.1946), superior inner (r = -0.2205), temporal inner (r = -0.1755), and inferior inner (r = -0.2448) S5 Table. Nasal (r = 0.1863) and nasal inferior (r = 0.1924) disc segments were significantly positively correlated while the temporal sector was negatively correlated (r = -0.2365) S6 Table.

Discussion and conclusion

SD OCT has revolutionised the diagnostic and prognostic capabilities for a number of ophthalmic conditions, including diabetic macular oedema, glaucoma, age-related macular degeneration and compressive optic neuropathy [10, 11]. Normative databases provide the reference values against which to compare cases of disease states. Although several studies report the normative data for SD OCT, [12–14] to the author's knowledge, no data exist for SD OCT that

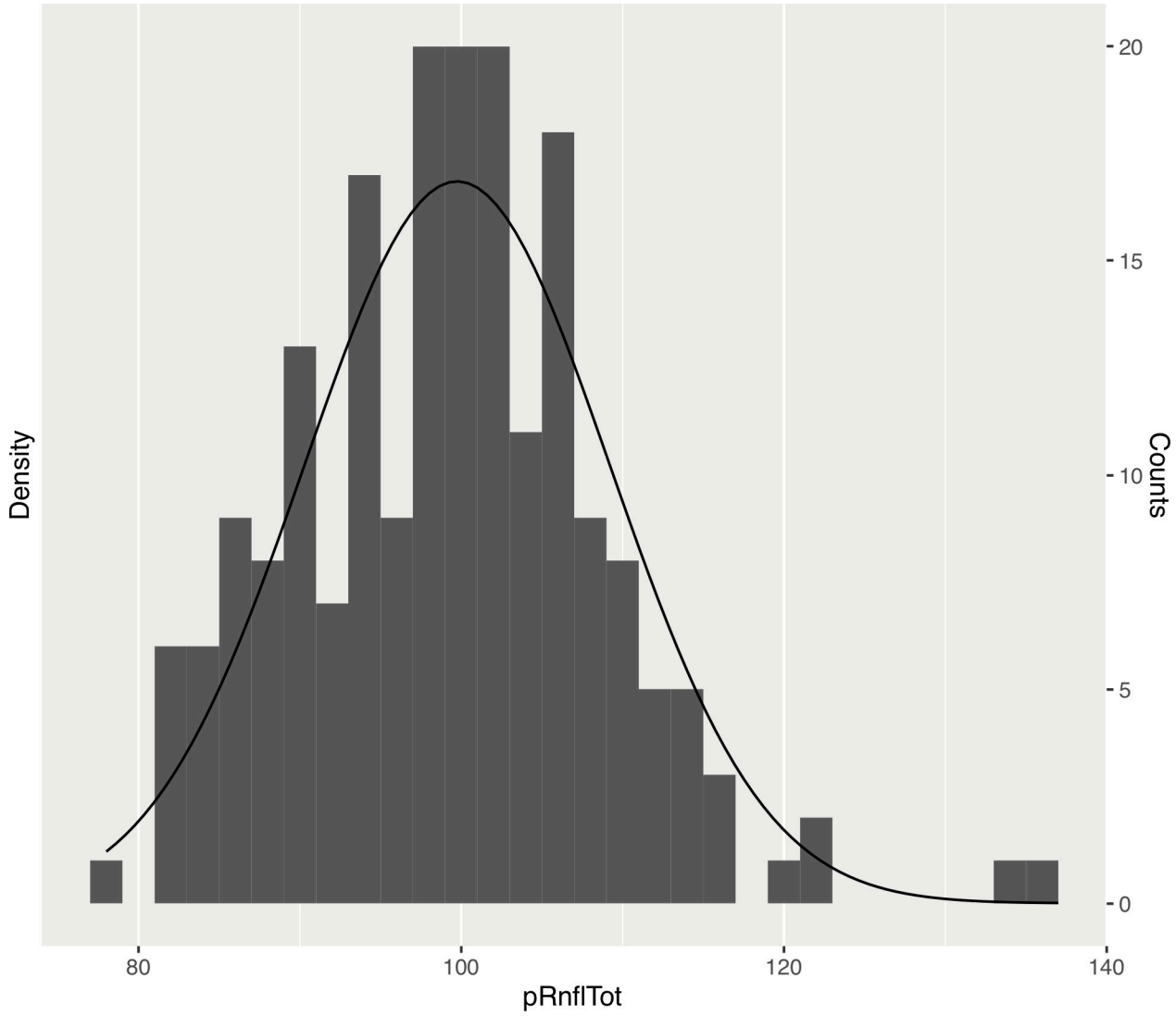

Fig 2. Histogram and fitted normal distribution curve of mean peripapillary retinal nerve fibre layer thickness values.

https://doi.org/10.1371/journal.pone.0253720.g002

includes both macular GCL and peripapillary RNFL scans at the A-scan level. Normative values presented in this study were comparable to those previously reported. Grover et al. found a mean central retinal thickness of 270.2 μm in a Caucasian population, Nieves-Moreno et al. 278.2 μm in a Caucasian population and Appukutan et al. 260.1 μm in an Indian population. Mean central retinal thickness in this study ranged between 270.17–280.15 μm. The A-scan is a single point of interrogation on the retina that represents the most basic unit of measurement data in the OCT. Equivalent A-scans represent the same anatomical location across patients. The comparison of A-scan measurements between patients is a more precise analysis than the standard ETDRS grid, which is based on averaged A-scan values across the segments. In the advent of analytical methodologies, such as artificial intelligence and machine learning, it is becoming increasingly possible to use larger volumes of data. The primary purpose of reporting normative A-scans is to facilitate further research into patterns of disease development at the retina beyond the confines of standardised grids, such as ETDRS, using such methodologies.

Table 3. Female regression coefficient in multivariate analysis controlling for age with macular sectorial thickness values as outcome.

Sector	Retina	p	mRNFL	p	GCL	p	IPL	p
Volume	−0.175751	***	−0.0112461		−0.0309332	*	−0.0121464	
Centre	−14.58119	***	−1.287385	***	−2.741456	***	−2.84705	***
Nasal inner	−11.15093	***	−0.86165	*	−2.44177	**	−1.23396	*
Nasal outer	−5.82186	**	−0.602074		−0.34252		0.09550	
Superior inner	−10.07472	***	−0.92011		−1.82976	**	−1.00703	*
Superior outer	−2.88614		0.97539		−0.51977		0.02971	
Temporal inner	−10.548601	***	−0.503470	*	−3.26108	***	−1.68946	**
Temporal outer	−4.83874	*	−0.39463		−1.01023		−0.97755	
Inferior inner	−10.35359	***	−1.438830	**	−1.97374	**	−1.07487	*
Inferior outer	−4.99137	*	−0.33538		−0.37526		−0.13309	

P-values are coded as:

***<0.001

**<0.01 and

*<0.05.

https://doi.org/10.1371/journal.pone.0253720.t003

Table 4. Macular retinal thickness distribution by age group, showing mean, first, fifth and 95th percentile values for each segment.

Retina	18–33				34–50				51–68				69–88			
		Percentile				Percentile				Percentile				Percentile		
	x̄	1st	5th	95th	x̄	1st	5th	95th	x̄	1st	5th	95th	x̄	1st	5th	95th
Volume	8.74	7.99	8.11	9.13	8.76	7.77	8.22	9.27	8.59	8.12	8.16	9.45	8.48	7.66	7.71	9.02
Centre	270.56	228.5	239.3	306.8	280.50	228.6	246.1	308.0	279.05	220.7	237.0	320.2	270.17	233.0	240.0	305.4
Nasal inner	348.29	321.0	327.0	369.7	353.31	314.0	329.0	378.0	345.77	319.7	324.2	379.2	342.45	315.6	317.4	371.6
Nasal outer	321.37	294.6	298.1	341.9	319.76	280.4	298.1	338.0	312.86	283.0	293.6	343.6	308.34	278.6	280.0	333.6
Superior inner	343.29	254.7	320.1	368.3	351.45	310.1	334.1	375.0	342.33	312.0	320.4	369.2	339.69	308.6	311.2	365.8
Superior outer	302.37	272.0	276.7	321.8	301.40	269.5	285.0	320.0	296.14	273.7	278.8	322.6	291.38	259.1	262.8	310.6
Temporal inner	329.56	300.0	305.1	352.9	337.15	295.6	318.0	360.9	330.67	302.2	304.8	362.6	327.41	299.1	302.0	346.2
Temporal outer	286.73	257.5	267.1	300.5	286.18	251.7	263.1	304.0	282.26	263.0	265.8	315.0	278.62	244.1	247.8	299.2
Inferior inner	343.35	315.1	320.2	362.9	347.48	309.6	328.0	370.9	339.61	316.0	316.8	371.0	338.31	309.4	314.2	361.2
Inferior outer	292.69	258.1	266.1	309.4	291.69	266.8	272.0	308.0	286.37	264.1	268.4	314.2	282.48	253.3	255.6	303.2

https://doi.org/10.1371/journal.pone.0253720.t004

Table 5. Macular retinal nerve fibre layer thickness distribution by age group, showing mean, first, fifth and 95th percentile values for each segment.

RNFL	18–33				34–50				51–68				69–88			
		Percentile				Percentile				Percentile				Percentile		
	x̄	1st	5th	95th	x̄	1st	5th	95th	x̄	1st	5th	95th	x̄	1st	5th	95th
Volume	0.95	0.77	0.81	1.12	0.96	0.74	0.76	1.16	0.94	0.75	0.78	1.11	1.01	0.79	0.88	1.16
Centre	12.42	8.0	9.0	16.0	12.98	6.6	10.0	16.0	12.91	8.6	9.0	16.2	12.41	8.0	8.8	15.0
Nasal inner	22.06	17.5	19.0	26.0	22.31	17.0	18.0	27.0	21.96	17.0	18.0	27.0	22.69	18.0	18.4	28.0
Nasal outer	51.73	39.0	43.0	65.0	51.44	38.0	38.0	69.9	48.79	29.1	38.8	58.8	53.24	25.5	40.6	64.0
Superior inner	25.54	19.5	21.6	31.4	26.02	19.6	20.1	32.0	25.28	19.6	20.8	31.2	27.45	20.8	23.0	35.2
Superior outer	38.15	27.5	31.1	45.0	39.26	28.6	30.1	50.8	37.68	26.0	28.6	45.6	41.62	30.4	34.4	50.8
Temporal inner	17.56	15.0	16.0	19.0	17.90	16.0	16.0	20.0	18.37	16.0	16.0	21.2	18.38	16.3	17.0	20.6
Temporal outer	18.73	16.0	17.0	20.0	18.77	16.6	17.0	21.0	20.39	16.6	17.0	23.0	21.07	19.0	19.0	23.0
Inferior inner	26.37	22.0	23.0	31.0	26.53	19.0	21.1	34.0	26.42	20.1	22.0	31.6	27.00	22.3	23.0	32.6
Inferior outer	42.27	30.0	32.0	49.0	41.50	30.2	32.0	53.0	41.79	30.0	31.8	53.2	42.72	33.0	33.4	51.2

https://doi.org/10.1371/journal.pone.0253720.t005

Table 6. Macular ganglion cell layer thickness distribution by age group, showing mean, first, fifth and 95th percentile values for each segment.

GCL	18–33				34–50				51–68				69–88			
		Percentile				Percentile				Percentile				Percentile		
	$\bar{x}$	1st	5th	95th	$\bar{x}$	1st	5th	95th	$\bar{x}$	1st	5th	95th	$\bar{x}$	1st	5th	95th
Volume	1.10	0.88	0.95	1.23	1.12	0.89	0.99	1.25	1.06	0.89	0.93	1.22	1.04	0.84	0.90	1.13
Centre	16.00	9.5	10.0	24.5	16.55	7.2	10.1	23.0	15.33	8.0	8.0	21.2	14.45	8.3	9.0	22.0
Nasal inner	54.10	39.1	46.7	59.9	54.69	41.2	46.0	62.0	51.32	37.5	45.0	58.2	51.79	39.4	43.4	58.0
Nasal outer	38.77	31.5	34.0	43.0	38.65	31.2	32.1	44.0	37.26	30.1	31.8	43.0	35.52	29.3	30.0	40.0
Superior inner	53.96	41.1	48.0	60.5	55.08	43.2	48.1	63.0	51.49	40.1	44.0	59.0	51.79	40.7	45.0	57.0
Superior outer	35.13	28.0	30.0	41.0	35.06	28.6	29.1	39.0	33.95	29.0	29.0	40.2	32.45	27.6	29.0	36.0
Temporal inner	47.94	30.5	38.7	56.5	50.63	38.0	40.1	58.0	46.68	34.7	39.2	54.0	47.03	33.0	38.4	54.6
Temporal outer	36.85	25.5	30.6	44.0	37.35	29.6	30.1	44.9	34.30	28.0	29.0	40.4	34.62	27.3	28.0	40.2
Inferior inner	53.60	42.1	47.6	60.0	54.21	43.4	47.0	63.0	50.96	42.2	44.0	58.4	51.55	40.2	46.0	57.2
Inferior outer	33.83	28.0	28.0	38.5	33.92	25.0	26.2	38.0	32.26	26.6	27.8	36.2	32.07	26.6	28.0	36.6

https://doi.org/10.1371/journal.pone.0253720.t006

Table 7. Macular inner plexiform layer thickness distribution by age group, showing mean, first, fifth and 95th percentile values for each segment.

IPL	18–33				34–50				51–68				69–88			
		Percentile				Percentile				Percentile				Percentile		
	$\bar{x}$	1st	5th	95th	$\bar{x}$	1st	5th	95th	$\bar{x}$	1st	5th	95th	$\bar{x}$	1st	5th	95th
Volume	0.91	0.79	0.80	1.03	0.91	0.71	0.81	0.99	0.87	0.73	0.77	1.01	0.86	0.72	0.76	0.93
Centre	21.15	14.0	15.0	27.9	22.24	13.6	15.1	28.0	21.53	14.6	15.8	27.2	20.90	15.3	16.0	26.0
Nasal inner	44.12	34.5	39.0	50.0	44.35	35.6	38.1	50.0	42.21	35.1	37.0	48.0	42.07	33.4	37.4	46.0
Nasal outer	29.75	24.5	25.6	34.0	29.31	22.0	24.1	33.0	28.21	22.6	23.8	33.0	26.90	22.0	22.4	30.6
Superior inner	42.58	34.5	37.1	47.0	42.82	35.8	38.0	49.0	40.25	33.1	34.8	46.2	40.24	34.0	34.8	43.6
Superior outer	28.87	23.5	25.0	33.0	28.10	21.6	24.0	32.0	27.28	23.0	23.8	33.0	26.38	22.3	23.4	29.6
Temporal inner	42.17	30.6	35.6	48.5	43.16	34.6	38.0	49.0	41.16	33.7	35.8	47.2	41.07	32.1	35.8	45.0
Temporal outer	32.52	26.5	27.6	36.5	32.44	24.2	27.0	37.0	30.77	25.0	26.8	36.2	30.79	26.3	27.0	34.6
Inferior inner	42.46	35.0	38.0	47.5	42.35	34.6	37.0	47.0	40.00	34.1	35.8	45.0	40.69	34.6	36.0	44.6
Inferior outer	27.44	22.0	23.0	32.0	27.29	20.0	20.2	31.0	25.91	20.6	22.0	30.0	26.10	22.3	23.0	29.6

https://doi.org/10.1371/journal.pone.0253720.t007

Table 8. Retinal nerve fibre layer disc distribution by age group, showing mean, first, fifth and 95th percentile values for each segment.

Disc	18–33				34–50				51–68				69–88			
		Percentile				Percentile				Percentile				Percentile		
	$\bar{x}$	1st	5th	95th	$\bar{x}$	1st	5th	95th	$\bar{x}$	1st	5th	95th	$\bar{x}$	1st	5th	95th
Total	99.96	82.5	86.1	113.5	101.34	83.6	87.0	120.8	98.42	82.0	83.8	112.0	98.55	79.7	84.8	109.2
Nasal superior	114.19	69.6	85.8	145.7	110.10	84.1	88.1	135.0	111.79	72.1	78.0	148.0	107.45	73.6	78.6	144.8
Nasal	74.90	48.5	50.6	103.3	78.39	50.8	57.0	99.9	76.02	53.7	56.8	95.0	79.79	58.1	63.4	100.8
Nasal inferior	111.96	61.5	71.2	149.8	115.85	70.0	79.0	152.7	112.68	75.6	81.4	157.2	112.48	77.5	84.8	153.0
Temporal superior	139.71	99.1	115.0	164.5	143.03	115.8	120.1	171.8	133.58	93.6	106.8	156.4	132.79	103.7	108.4	152.2
Temporal	71.37	51.5	54.7	92.1	69.37	57.2	58.0	84.0	68.89	52.8	57.0	83.2	70.14	46.2	57.0	90.2
Temporal inferior	141.50	91.0	119.6	166.9	145.55	117.1	120.1	183.7	139.56	89.3	111.2	173.4	135.28	115.3	116.4	149.2

https://doi.org/10.1371/journal.pone.0253720.t008

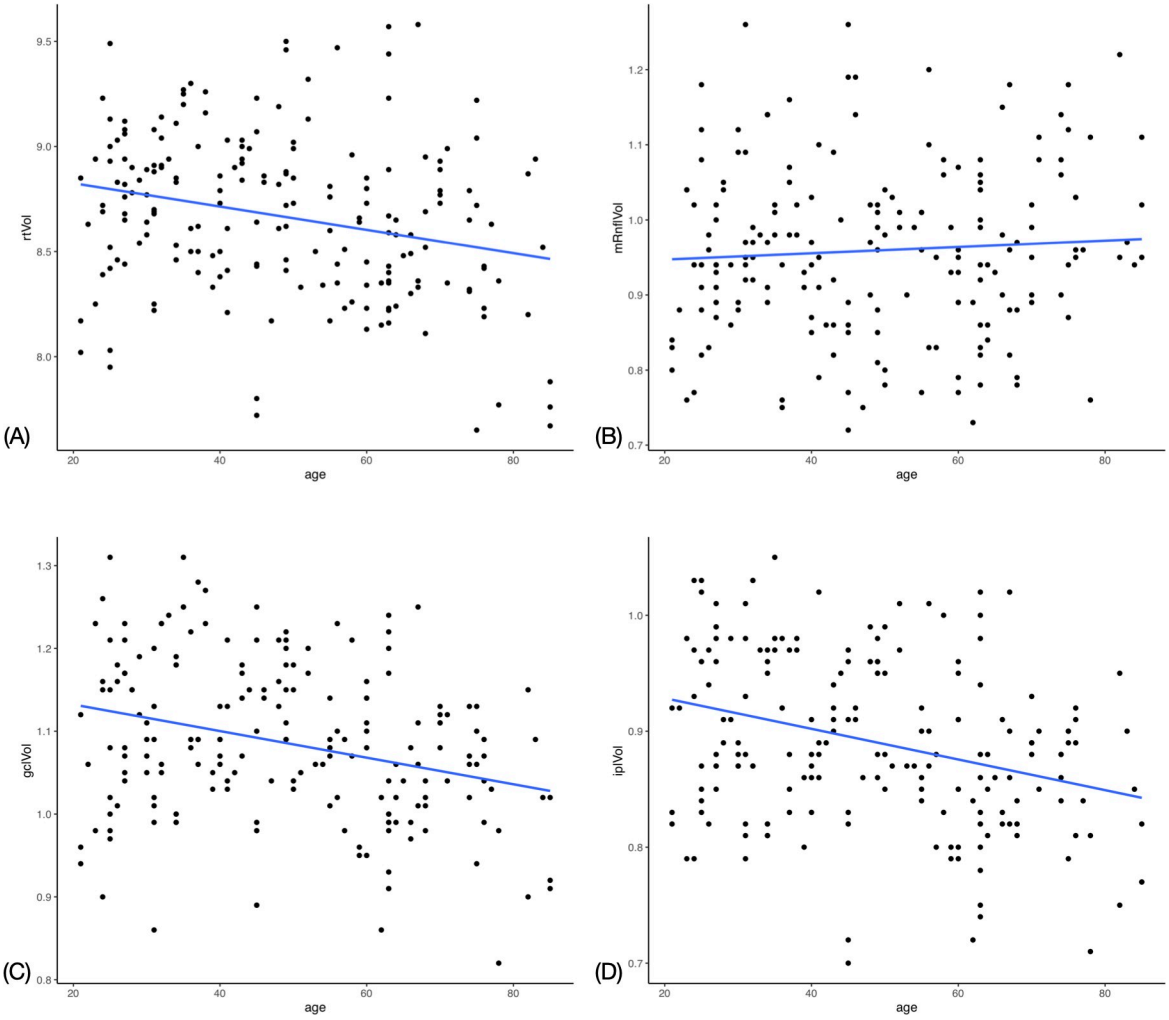

Fig 3. Scatter plot with trend line for macular optical coherence tomography measurements against age. (A) Total retinal volume. (B) Retinal nerve fibre layer volume. (C) Ganglion cell layer volume. (D) Inner plexiform layer volume.

https://doi.org/10.1371/journal.pone.0253720.g003

In the creation of a normative database, inclusion and exclusion criteria must be carefully considered to realistically represent the distribution of normal and diseased populations of interest. This study aimed to create a normative dataset of OCT scans for ongoing research of glaucoma and compressive optic neuropathies within the metropolitan region of Melbourne, Australia. An ethnically diverse population was used to represent the target population. All nine of the broad ethnic groups present in Australia were represented in our study population.

Proportions of four of the nine groups were significantly different compared to the known proportions in Melbourne. The ethnic groups used in this study were extracted from population census data that were designed according to political and geographical boundaries. This may have caused the grouping of some participants with differing genetic influences on their retinal structure. For example, the Americas ethnic group included both African American and Caucasian American people that have been shown to have different OCT measurements [15, 16]. This was an unavoidable limitation set by the Australian census groups [17].

This study found a negative association between age and macular thickness, which has been previously demonstrated. All the sectors of the ETDRS grid have been reported to be negatively associated with increasing age, except for the central 1 mm of the retina [13, 18–20].

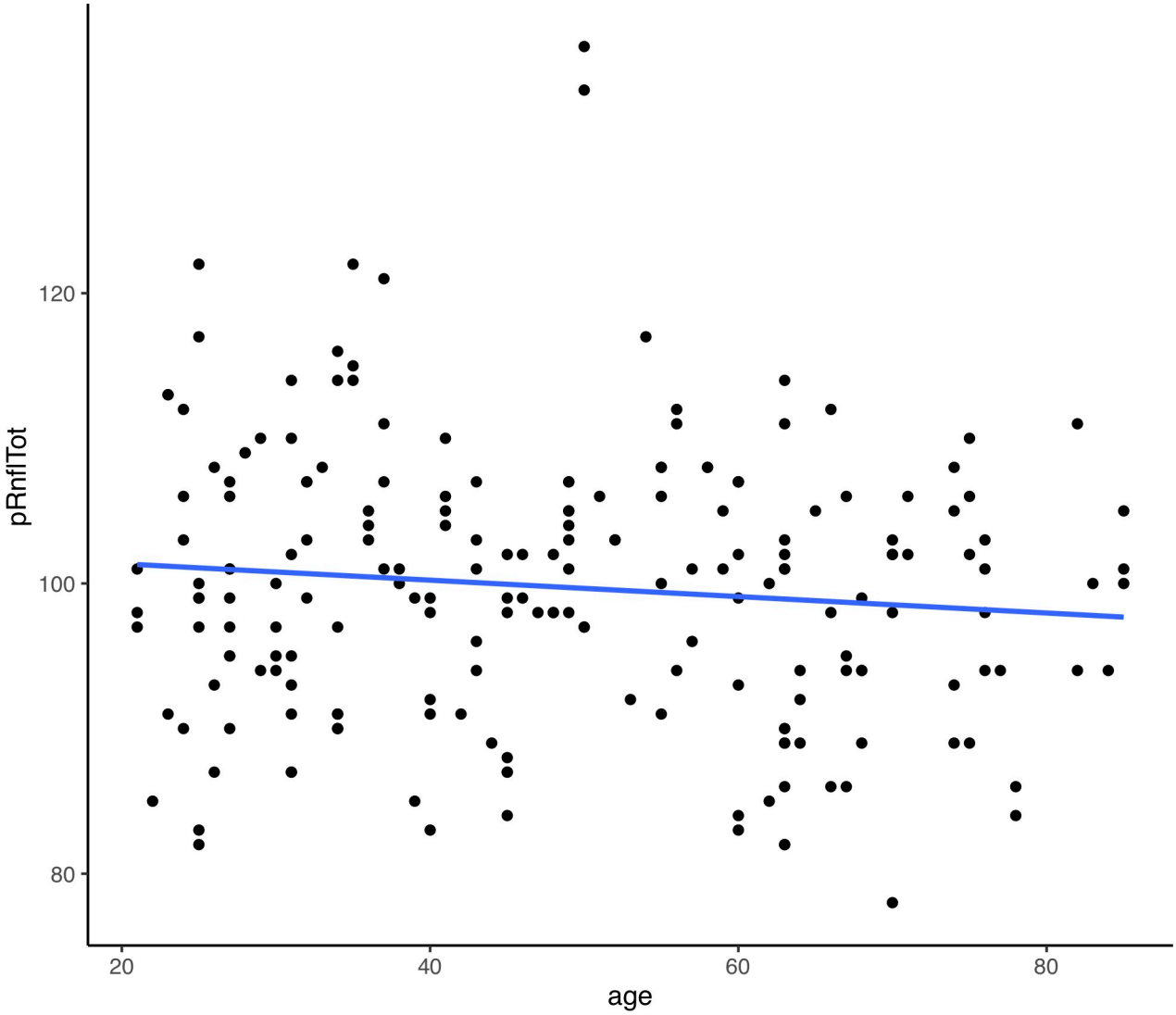

Fig 4. Scatter plot with trend line for mean peripapillary retinal nerve fibre layer thickness against age.

https://doi.org/10.1371/journal.pone.0253720.g004

This study is consistent with these findings; however, the negative correlation found in the temporal inner and inferior inner segments was found not to be statistically significant. Similar to other studies, the central area had almost no association (r = 0.00899, p = 0.9008). This study identified that the GCL and IPL thickness and volume for all the sectors (excluding the centre for the IPL) decreased with age. This was in keeping with findings from previous studies [13, 18, 21].

A statistically significant positive correlation was found between increasing age and temporal inner RNFL thickness (r = 0.1929, p = 0.0062). Similarly, Nieves-Moreno et al. found a positive correlation between temporal inner RNFL and age (r = 0.256, p = <0.001).[11] No other significant correlations were found between RNFL volume or thickness and age in this study. Given that the temporal inner is the thinnest RNFL sector, we postulate that it would be proportionally the most affected by an increasing thickness observed in the internal limiting membrane with age and, therefore, correlate positively with age. Males were found to have a

significantly higher RT, RNFL, GCL and IPL thickness than females. This was most evident in the inner layers, which is similar to the OCT results reported in other studies [13, 18].

It is well reported that the macula is thinner as the degree of myopia increases, [22–25] which is consistent with the findings from this study. Interestingly however, the correlation in this study suggests that the central RNFL increased with the degree of myopia. This was similar to a previous study which found an increase in foveal thickness with increasing myopia [22]. It has been proposed that the thinning in myopes is due to the increased axial length resulting in mechanical stretching of the sclera and pan retinal thinning. As well as this, the stretching and flattening of the ILM and centripetal force on the posterior vitreous may result in elevation of the fovea, which may account for the results from this study.

The Limitations of this study include its retrospective design, which led to missing variables including the axial length, refraction, and a non-standardised approach to the clinical examination that may have affected the OCT measurements. This study provides normal baseline data for the comparison of various macular diseases. These data will also be used to monitor patients with glaucoma and compressive optic neuropathy at The RMH.

Supporting information

S1 Table. Female regression coefficient in multivariate analysis controlling for age with peripapillary retinal nerve fibre layer sectoral thickness values as outcome.
(DOCX)

S2 Table. Mean volumes by gender.
(DOCX)

S3 Table. Regression analysis of layer thickness (μm) against age (years) and p-value for each macular segment.
(DOCX)

S4 Table. Regression analysis of layer thickness (μm) against age (years) and p-value for each disc segment.
(DOCX)

S5 Table. Regression analysis of layer thickness (μm) against refractive error (dioptres) and p-value for each macular segment.
(DOCX)

S6 Table. Regression analysis of layer thickness (μm) against refractive error (dioptres) and p-value for each disc segment.
(DOCX)

Acknowledgments

Amanda Rebbechi–medial photographer; Joss Dimock–medical photographer, Debbie Curran–medical photographer

Author Contributions

Conceptualization: Joos Meyer, Andrew Symons.

Data curation: Joos Meyer, Roshan Karri.

Formal analysis: Joos Meyer.

Investigation: Joos Meyer.

Methodology: Joos Meyer, Andrew Symons.

Project administration: Joos Meyer.

Resources: Joos Meyer, Andrew Symons.

Supervision: Helen Danesh-Meyer, Kate Drummond, Andrew Symons.

Validation: Andrew Symons.

Visualization: Joos Meyer.

Writing – original draft: Joos Meyer.

Writing – review & editing: Helen Danesh-Meyer, Kate Drummond, Andrew Symons.

References

1. Huang D, Swanson E, Lin C, Schuman J, Stinson W, Chang W, et al. Optical coherence tomography. Science. 1991; 254(5035):1178–81. https://doi.org/10.1126/science.1957169 PMID: 1957169
2. Danesh-Meyer HV, Yap J, Frampton C, Savino PJ. Differentiation of Compressive from Glaucomatous Optic Neuropathy with Spectral-Domain Optical Coherence Tomography. Ophthalmology. 2014; 121 (8):1516–23. https://doi.org/10.1016/j.ophtha.2014.02.020 PMID: 24725827
3. Huang D, Swanson E, Lin C, Schuman J, Stinson W, Chang W, et al. Optical coherence tomography. Science. 1991; 254(5035):1178–81. https://doi.org/10.1126/science.1957169 PMID: 1957169
4. Group ETDRSR. Grading Diabetic Retinopathy from Stereoscopic Color Fundus Photographs—An Extension of the Modified Airlie House Classification. Ophthalmology. 1991; 98(5):786–806. PMID: 2062513
5. Early photocoagulation for diabetic retinopathy. ETDRS report number 9. Early Treatment Diabetic Retinopathy Study Research Group. Ophthalmology. 1991; 98(5 Suppl):766–85. PMID: 2062512
6. Röhlig M, Prakasam RK, Stüwe J, Schmidt C, Stachs O, Schumann H. Enhanced Grid-Based Visual Analysis of Retinal Layer Thickness with Optical Coherence Tomography. Information. 2019; 10 (9):266.
7. (ABS) AB of S. Australian Standard Classification of Cultural and Ethnic Groups (ASCCEG) [Internet]. n.d. Available from: https://www.abs.gov.au/ausstats/abs@.nsf/Previousproducts/1249.0Main%20Features12011?
8. R Development Core Team: A Language and Environment for Statistical Computing. Vienna, Austria: R Foundation for Statistical Computing; 2011.
9. Wickham H. ggplot2: Elegant Graphics for Data Analysis [Internet]. Springer-Verlag New York; 2016. Available from: https://ggplot2.tidyverse.org
10. Danesh-Meyer HV, Wong A, Papchenko T, Matheos K, Stylli S, Nichols A, et al. Optical coherence tomography predicts visual outcome for pituitary tumors. J Clin Neurosci. 2015; 22(7):1098–104. https://doi.org/10.1016/j.jocn.2015.02.001 PMID: 25891894
11. Adhi M, Duker JS. Optical coherence tomography—current and future applications. Curr Opin Ophthalmol. 2013; 24(3):213–21. https://doi.org/10.1097/ICU.0b013e32835f8bf8 PMID: 23429598
12. Grover S, Murthy RK, Brar VS, Chalam KV. Normative Data for Macular Thickness by High-Definition Spectral-Domain Optical Coherence Tomography (Spectralis). Am J Ophthalmol. 2009; 148(2):266–71. https://doi.org/10.1016/j.ajo.2009.03.006 PMID: 19427616
13. Nieves-Moreno M, Martínez-de-la-Casa JM, Cifuentes-Canorea P, Sastre-Ibáñez M, Santos-Bueso E, Sáenz-Francés F, et al. Normative database for separate inner retinal layers thickness using spectral domain optical coherence tomography in Caucasian population. Plos One. 2017; 12(7):e0180450. https://doi.org/10.1371/journal.pone.0180450 PMID: 28678834
14. Appukuttan B, Giridhar A, Gopalakrishnan M, Sivaprasad S. Normative spectral domain optical coherence tomography data on macular and retinal nerve fiber layer thickness in Indians. Indian J Ophthalmol. 2014; 62(3):316–21. https://doi.org/10.4103/0301-4738.116466 PMID: 24008793
15. Kelty PJ, Payne JF, Trivedi RH, Kelty J, Bowie EM, Burger BM. Macular Thickness Assessment in Healthy Eyes Based on Ethnicity Using Stratus OCT Optical Coherence Tomography. Investigative Opthalmology Vis Sci. 2008; 49(6):2668. https://doi.org/10.1167/iovs.07-1000 PMID: 18515595

16. Kashani AH, Zimmer-Galler IE, Shah SM, Dustin L, Do DV, Eliott D, et al. Retinal Thickness Analysis by Race, Gender, and Age Using Stratus OCT. Am J Ophthalmol. 2010; 149(3):496–502.e1. https://doi.org/10.1016/j.ajo.2009.09.025 PMID: 20042179

17. Realini T, Zangwill LM, Flanagan JG, Garway-Heath D, Patella VM, Johnson CA, et al. Normative Databases for Imaging Instrumentation. J Glaucoma. 2015; 24(6):480–3. https://doi.org/10.1097/IJG.0000000000000152 PMID: 25265003

18. Demirkaya N, Dijk HW van, Schuppen SM van, Abràmoff MD, Garvin MK, Sonka M, et al. Effect of Age on Individual Retinal Layer Thickness in Normal Eyes as Measured With Spectral-Domain Optical Coherence Tomography. Investigative Opthalmology Vis Sci. 2013; 54(7):4934. https://doi.org/10.1167/iovs.13-11913 PMID: 23761080

19. Manassakorn A, Chaidaroon W, Ausayakhun S, Aupapong S, Wattananikorn S. Normative database of retinal nerve fiber layer and macular retinal thickness in a Thai population. Jpn J Ophthalmol. 2008; 52(6):450–6. https://doi.org/10.1007/s10384-008-0538-6 PMID: 19089565

20. Appukuttan B, Giridhar A, Gopalakrishnan M, Sivaprasad S. Normative spectral domain optical coherence tomography data on macular and retinal nerve fiber layer thickness in Indians. Indian J Ophthalmol. 2014; 62(3):316–21. https://doi.org/10.4103/0301-4738.116466 PMID: 24008793

21. Repka MX, Quigley HA. The Effect of Age on Normal Human Optic Nerve Fiver Number and Diameter. Ophthalmology. 1989; 96(1):26–32. https://doi.org/10.1016/s0161-6420(89)32928-9 PMID: 2919049

22. Hwang YH, Kim YY. Macular thickness and volume of myopic eyes measured using spectral-domain optical coherence tomography. Clin Exp Optom. 2012; 95(5):492–8. https://doi.org/10.1111/j.1444-0938.2012.00749.x PMID: 22759271

23. Sato A, Fukui E, Ohta K. Retinal thickness of myopic eyes determined by spectralis optical coherence tomography. Brit J Ophthalmol. 2010; 94(12):1624. https://doi.org/10.1136/bjo.2009.165472 PMID: 20494914

24. Song WK, Lee SC, Lee ES, Kim CY, Kim SS. Macular Thickness Variations with Sex, Age, and Axial Length in Healthy Subjects: A Spectral Domain–Optical Coherence Tomography Study. Invest Ophth Vis Sci. 2010; 51(8):3913–8.

25. WAKITANI Y, SASOH M, SUGIMOTO M, ITO Y, IDO M, UJI Y. MACULAR THICKNESS MEASUREMENTS IN HEALTHY SUBJECTS WITH DIFFERENT AXIAL LENGTHS USING OPTICAL COHERENCE TOMOGRAPHY. Retin. 2003; 23(2):177–82. https://doi.org/10.1097/00006982-200304000-00007 PMID: 12707596